Transition from negative magnetoresistance behavior to positive behavior in $Co_{20}(Cu_{1-x}Ge_x)_{80}$ ribbons

J. He[a)] and Z. D. Zhang
Shenyang National Laboratory for Materials Science and International Centre for Materials Physics, Institute of Metal Research, Chinese Academy of Sciences, Shenyang 110016, People's Republic of China

J. P. Liu[b)] and D. J. Sellmyer
Department of Physics and Astronomy and Center for Materials Research and Analysis, University of Nebraska, Lincoln, Nebraska 68588-0113

(Received 26 October 2001; accepted for publication 9 January 2002)

We report a transition of the giant magnetoresistance (GMR) behavior in nanocrystalline $Co_{20}(Cu_{1-x}Ge_x)_{80}$ ribbons from negative to positive, as the semiconductor Ge substitutes for the Cu matrix. The growth of the hexagonal Co_3Ge_2 compound leads to a change of the physical origin of the GMR. The normal spin-dependent transport behavior in the CoCu granular system evolves into Coulomb blockade behavior of electronic tunneling in ribbons with a $Co/Co_3Ge_2/Co$ junctionlike configuration. © *2002 American Institute of Physics.* [DOI: 10.1063/1.1458682]

The (negative) giant magnetoresistance (GMR) effect has been observed in many structures such as antiferromagnetically coupled multiplayers,[1,2] magnetic granular systems,[3,4] and tunneling junctions.[5] Recently, research interest in the GMR effect has turned to hybrid ferromagnet–insulator and ferromagnet–semiconductor structures.[6–12] The enhancement of insulating characteristics in the nonmagnetic matrix causes the separation of metallic granules by a network of insulating boundaries and the appearance of Coulomb blockade, resulting in the increase of negative GMR.[8–11] The electronic transport behavior is thought to stem from spin-dependent tunneling.

In addition, several methods such as ion implantation[13,14] and molecular-beam epitaxy[15] were used to imbed magnetic Mn particles in semiconductor GaAs or Sb, leading to the behavior of positive magnetoresistance. The strong positive GMR in Mn-implanted GaAs films is correlated with the spacing of magnetic nanoparticles, while in MnSb films it originates from the Coulomb blockade of electronic tunneling. Here, we report on $Co_{20}(Cu_{1-x}Ge_x)_{80}$ ribbons showing the transition of magnetoresistance from negative to positive with substitution of the metallic matrix Cu by the semiconductor Ge. The formation of the Co_3Ge_2 compound results in the existence of $Co/Co_3Ge_2/Co$ junction-like configurations, which helps to explain the interesting GMR transition.

As-quenched $Co_{20}(Cu_{1-x}Ge_x)_{80}$ ($0 \leqslant x \leqslant 0.1$) ribbons, 25–30 μm thick and 1.2 mm wide, were fabricated by rapid quenching under argon atmosphere. The ribbons were annealed at 693, 723, 753, and 773 K for 20 min in 10^{-7} Torr. The microstructures were observed using a Philips EM 420 transmission electron microscope (TEM). The magnetization was measured by a superconducting quantum interference device (SQUID). Four-probe resistivity measurement was performed by a Lakeshore 7000 system. Typical TEM images of the ribbons are shown in Fig. 1. The phase separation after annealing makes 5–10 nm magnetic Co particles embed in the large Cu matrix for pure metallic $Co_{20}Cu_{80}$ ribbons [Fig. 1(a)]. As Ge content reaches 0.04–0.06, an elongated structure appears [Fig. 1(b)]. Analysis of x-ray and TEM diffraction patterns shows that the thin slices are the hexago-

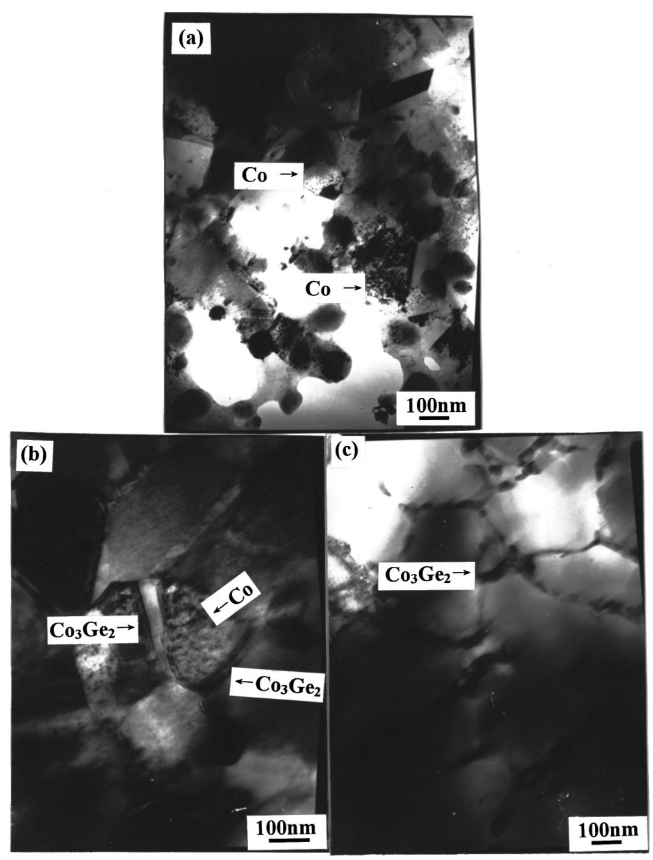

FIG. 1. Bright-field image obtained by transmission electron microscopy (TEM) of $Co_{20}(Cu_{1-x}Ge_x)_{80}$ granular ribbons annealed at 753 K for 20 min; (a) $x=0$, (b) $x=0.055$, and (c) $x=0.1$.

[a)]Also at: Department of Physics and Astronomy and Center for Materials Research and Analysis, University of Nebraska, Lincoln, NE 68588-0113; electronic mail: jun50543@yahoo.com

[b)]Also at: Institute for Micromanufacturing, Louisiana Technical University, Ruston, LA 71272.

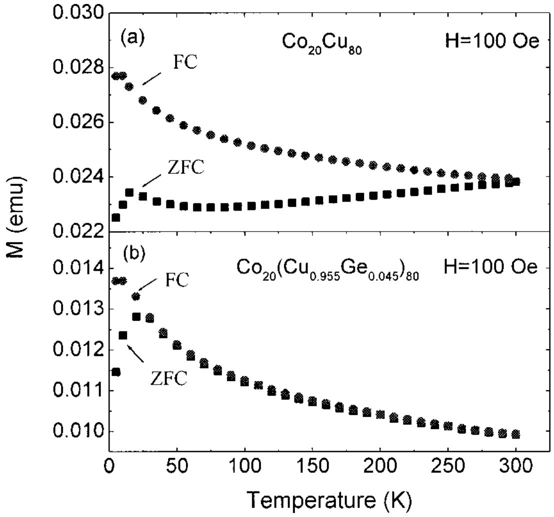

FIG. 2. Magnetization curves after zero-field cooling (ZFC) and field cooling (FC) for (a) $Co_{20}Cu_{80}$ and (b) $Co_{20}(Cu_{0.955}Ge_{0.045})_{80}$ ribbons annealed at 753 K, respectively. The applied field is 100 Oe.

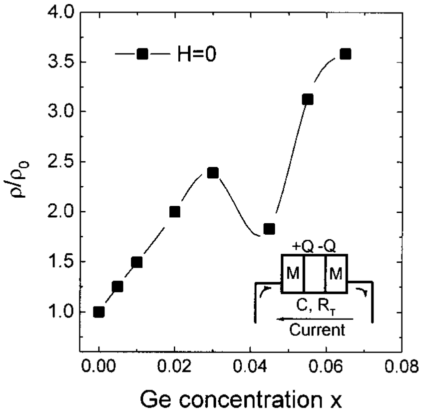

FIG. 4. Ge content dependence of normalized resistivity at zero magnetic field. ρ_0 denotes the resistivity of Ge-free ribbons. The inset is the sketch of the tunneling process in a single junction, in which C is capacitance, R_T is tunneling resistance, and Q is the charge on the pole plate.

nal Co_3Ge_2 compounds. With further increasing the Ge content, as shown in Fig. 1(c), the Co_3Ge_2 compound aggregates together in the interface of Cu clusters to form a network of boundaries. Co nanoparticles nearly disappear in the matrix, indicating that the formation of Co_3Ge_2 strongly restrains their growth.

Magnetization versus temperature for zero-field-cooled (ZFC) and field-cooled (FC) curves are shown in Figs. 2(a) and 2(b) for $Co_{20}Cu_{80}$ and $Co_{20}(Cu_{0.955}Ge_{0.045})_{80}$ annealed ribbons, respectively. The ZFC and FC curves of the $Co_{20}Cu_{80}$ ribbons are separated at all temperatures. By contrast, the ZFC and ZC curves of the $Co_{20}(Cu_{0.955}Ge_{0.045})_{80}$ ribbons nearly overlap above the spin-freezing point. In fact, the effect of the applied field to the magnetic Co moment in the pure Cu matrix is much stronger than that in the CuGe matrix due to the decrease of the quantity of magnetic Co particles with Ge substitution for Cu [in Fig. (c)]. Thus, the separation of FC and ZFC curves for $Co_{20}Cu_{80}$ is more obvious than that for $Co_{20}(Cu_{0.955}Ge_{0.045})_{80}$, which is in agreement with Ref. 16.

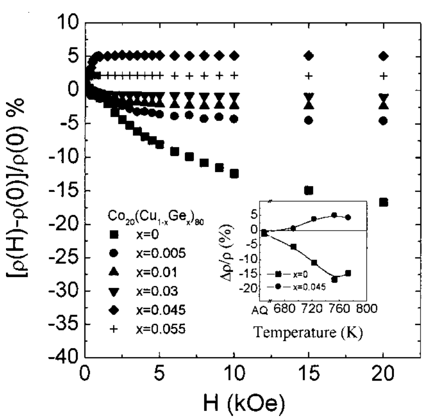

FIG. 3. Transition of magnetoresistance behavior from negative to positive with substitution of Cu by Ge for $Co_{20}(Cu_{1-x}Ge_x)_{80}$ granular ribbons annealed at 753 K for 20 min. The inset shows the evolvement of positive GMR ratio obtained at $H=20$ kOe for as-quenched and annealed (at 693, 723, 753, and 773 K) $Co_{20}(Cu_{0.955}Ge_{0.045})_{80}$ ribbons. The negative ratio for $Co_{20}Cu_{80}$ ribbons is also shown. The magnetic field is parallel to the longitudinal direction of the ribbons.

As shown in Fig. 3, a clear GMR transition exists with Ge substitution for Cu. The GMR ratio $[\rho(H)\text{-}\rho(0)]/\rho(0)$ reaches about -16% in the Ge-free ribbons. This negative GMR drops rapidly in the Ge-containing ribbons and the transition from negative to positive takes place as the Ge content increases to 0.045. In contrast to the negative GMR effect, the positive GMR effect $(+5\%)$ saturates at a lower magnetic field (2.5 kOe) with the sensitivity of 10.5%/kOe. The changes of the GMR ratio with annealing temperature for $Co_{20}Cu_{80}$ and $Co_{20}(Cu_{0.955}Ge_{0.045})_{80}$ ribbons are exhibited in the inset of Fig. 3. All annealed $Co_{20}(Cu_{0.955}Ge_{0.045})_{80}$ ribbons present the positive GMR. Clearly, the electronic transport mechanism in the ribbons has been changed with Ge substitution for Cu.

The negative GMR effect can be described by the attenuation of spin-dependent scattering due to the alignment of magnetic particles by the external magnetic field. The effect declines with decreasing the amount of the Co particles. However, the existence of Co_3Ge_2 compounds in the Cu matrix changes the conductive homogeneities due to its high resistance. The electronic tunneling should contribute to the electronic transport since many nanosize $Co/Co_3Ge_2/Co$ junctionlike configurations are distributed widely [see Fig. 1(b)]. As usual, at low temperatures electronic tunneling in the junctions can be restrained by a large charging energy change at a certain range of charge Q, which is called the Coulomb blockade. This effect can enhance the negative GMR effect in a certain condition.[9,10] However, in $Co_{20}(Cu_{1-x}Ge_x)_{80}$ annealed ribbons, the positive GMR behaviors are observed with increasing x. Furthermore, the positive GMR ratio declines to zero with progressive substitution of Cu by Ge, as shown in Fig. 3. It seems unreasonable to explain this transition by the traditional spin-dependent tunneling mechanism. Figure 4 shows that the resistivity indeed enhances with Ge substitution when $x < 0.03$. As x becomes larger than 0.03, ρ suddenly decreases, reminding us of a junction tunneling independent of electronic spins. Basically, a metal–insulator–metal junction with a bias current I, as shown in the inset of Fig. 4, can be described by charge Q and the magnitude of tunneling electrons n. The electron tunneling leads to the change of static potential:[12]

$$\Delta E^{\pm}=\frac{Q^2}{2C}-\frac{(Q\mp e)^2}{2C}=\pm\frac{e}{C}\left(Q\mp\frac{e}{2}\right). \quad (1)$$

When the temperature is much lower, tunneling can take place only if the energy of the system decreases $(\Delta E>0)$. Namely, the Coulomb blockade appears when charge Q is at a given range: $-0.5e<Q<0.5e$. Due to the growth of hexagonal Co_3Ge_2 slices, capacitance C of the $Co/Co_3Ge_2/Co$ junctions becomes larger so that charge Q on the pole plate increases. When Q surpasses threshold $e/2$, tunneling occurs in the junctions, resulting in the drop of resistivity, as shown in Fig. 4. The applied magnetic field makes the Coulomb gap $(e/2C)$ larger by alignment of Co nanoparticles so that to some extent the junction is restored and the Coulomb blockade effect acts. This seems to cause the positive GMR behavior. When $x>0.06$, more Co_3Ge_2 phases form in the ribbons as network-like insulating boundaries while the amount of Co particles decreases in the matrix. On the other hand, the decrease of charging energy $E_c=e^2/2C$, due to the further increase of capacitance C, destroys the condition that the charging energy must be much larger than heat fluctuation k_BT. Thus, it is difficult for the Coulomb blockade to occur when the Ge content is high. Both of these lead to the decrease of the positive GMR effect.

In conclusion, we have presented experimental evidence for the transition of the GMR effect from negative to positive induced by the growth of a Co_3Ge_2 phase in the $Co_{20}(Cu_{1-x}Ge_x)_{80}$ ribbons. The interaction between the spin-dependent scattering and the Coulomb blockade of electronic tunneling directly demonstrates the nature of the transition. The interesting GMR transition provides insight into exploring the spin-dependent phenomenon in the semimetal matrix and will be of technological importance in the development of magnetoelectronic research.

This work was supported by the National Natural Science Foundation of China under Grant No. 59725103 and the U.S. NSF under Grant No. INT-9812082. The authors gratefully acknowledge the help of Professor Li-zhi Cheng in the manufacture of the ribbons and Professor Michael O'Shea and Dr. Bao-zhi Cui for the SQUID experiments.

[1] M. N. Baibich, J. M. Broto, A. Fert, F. Nguyen van Dau, F. Petroff, P. Etienne, G. Creuzet, A. Friedrich, and J. Chazelas, Phys. Rev. Lett. **61**, 2472 (1988).
[2] S. S. Parkin, N. More, and K. P. Roche, Phys. Rev. Lett. **64**, 2304 (1990).
[3] J. Q. Xiao, J. Jiang, and C. L. Chien, Phys. Rev. Lett. **68**, 3749 (1992).
[4] S. M. Jordarn, R. Schad, A. M. Keen, M. Bischoff, D. S. Schmool, and H. van Kempen, Phys. Rev. B **59**, 7350 (1999).
[5] T. Miyazaki and N. Tezuka, J. Magn. Magn. Mater. **139**, L231 (1995).
[6] G. A. Prinz, Science **250**, 1092 (1990).
[7] H. Ohno, Science **281**, 951 (1998).
[8] H. Akinaga, J. De Boeck, G. Borghs, S. Miyanishi, A. Asmitsu, W. Van-Roy, Y. Tomioka, and L. H. Kuo, Appl. Phys. Lett. **72**, 3368 (1998).
[9] S. Mitani, S. Takahashi, K. Takanashi, K. Yakushiji, S. Maekawa, and H. Fujimori, Phys. Rev. Lett. **81**, 2799 (1998).
[10] S. Mitani, K. Takanashi, and K. Yakushiji, Mater. Sci. Eng., B **84**, 120 (2001).
[11] K. Yakushiji, S. Mitani, K. Takanashi, S. Takahashi, S. Maekawa, H. Imamura, and H. Fujimori, Appl. Phys. Lett. **78**, 515 (2001).
[12] H. Grabert and M. Devoret, *Single Charge Tunneling* (Plenum, New York, 1992).
[13] P. J. Wellmann, J. M. Garcia, J. L. Feng, and P. M. Petroff, Appl. Phys. Lett. **73**, 3291 (1998).
[14] Sh. U. Yuldashev, Y. Shon, Y. H. Kwon, D. J. Fu, D. Y. Kim, H. J. Kim, and T. W. Kang, J. Appl. Phys. **90**, 3004 (2001).
[15] H. Akinaga, M. Mizuguchi, K. Ono, and M. Oshima, Appl. Phys. Lett. **76**, 357 (2000).
[16] P. Jena, S. N. Khanna, and B. K. Rao, *Cluster and Nanostructure Interfaces* (1999).